Active bound states arising from transiently nonreciprocal pair interactions

Luca Cocconi,[1,2,3,*] Henry Alston,[1,*] and Thibault Bertrand[1,†]
[1]Department of Mathematics, Imperial College London, South Kensington, London SW7 2AZ, United Kingdom
[2]The Francis Crick Institute, London NW1 1AT, United Kingdom
[3]Max Planck Institute for Dynamics and Self-Organization (MPIDS), 37077 Göttingen, Germany

(Received 16 April 2023; accepted 22 August 2023; published 11 October 2023)

Static nonreciprocal forces between particles generically drive persistent motion reminiscent of self-propulsion. Here, we demonstrate that reciprocity-breaking fluctuations about a reciprocal mean coupling strength are sufficient to generate this behavior in a minimal two-particle model, with the velocity of the ensuing *active* bound state being modulated in time according to the nature of these fluctuations. To characterize the ensuing nonequilibrium dynamics, we derive exact results for the time-dependent center of mass mean-square displacement and average rate of entropy production for two simple examples of discrete- and continuous-state fluctuations in one dimension. We find that the resulting dimer can exhibit unbiased persistent motion akin to that of an active particle, leading to a significantly enhanced effective diffusivity.

DOI: 10.1103/PhysRevResearch.5.043032

I. INTRODUCTION

Newton's third law states that microscopic forces respect action-reaction symmetry; yet many examples of nonreciprocal effective interactions have been identified in living and reactive systems. These range from classical predator-prey [1,2] and activator-inhibitor [3] models to interactions mediated by a nonequilibrium medium [4–7]. Nonreciprocity also arises in systems with asymmetric information flows [8] and memory effects [9,10].

The breaking of reciprocal symmetry in many-body systems generates fundamentally nonequilibrium dynamics at the collective scale [11–15]. Most strikingly, an imbalance in effective physical forces between particles can drive persistent motion, reminiscent of self-propulsion [13]. Motile particle clusters [5–7,16–18] and self-propelling droplets [19] have been experimentally realized in systems with constant nonreciprocal couplings. Furthermore, the thermodynamic implications of reciprocity breaking were studied in several theoretical models [9,13].

In principle, the introduction of temporal fluctuations in nonreciprocal interactions would provide a mechanism to control the propulsion speed and direction of the ensuing dynamical phase. Such fluctuations may, for instance, arise generically in physical systems through dynamic properties in the nonequilibrium medium that mediates interactions. Examples include the concentration of so-called *doping agents* in chemically interacting particle systems [7] or of a surfactant in an experimental setup of self-propelled liquid droplets which allowed for the reversal of the direction of motion [19]. In recent studies, active motion was shown to emerge from the application of a time-dependent external magnetic field on nanoparticle dimers [20] and many magnetic microdisks, where effective nonreciprocal interactions also drive collective motion that inherently breaks chiral symmetry [21].

Fluctuating *reciprocal* interactions in many-body systems lead to nonequilibrium, dissipative structures [22] and dynamics [23]. We have previously studied the thermodynamic implications of these interactions in Ref. [24], where we obtained analytically the nonzero average rate of entropy production in a variety of minimal setups. Though static nonreciprocal couplings have been studied in a similar manner [9,15], a complete thermodynamically consistent picture for dynamic, nonreciprocal interactions is key to the analysis of important reactive, active, and living processes.

Here, we consider a minimal two-particle model of fluctuating nonreciprocal forces. We fix the interactions to be reciprocal on average; yet we let them break the action-reaction principle transiently through temporal fluctuations in the interaction strengths, isolating the impact of reciprocal-symmetry-breaking fluctuations on the collective dynamics and thermodynamic properties of the system. We show that these systems can exhibit collective motion reminiscent of active particles; thus we refer to the resulting two-particle dimers as *active bound states*. For particular choices of the fluctuations and in the presence of steric repulsion, the ensuing dynamics can be mapped onto those of *run-and-tumble* [25–27] and *active Ornstein-Uhlenbeck* [28,29] particles.

II. MINIMAL TWO-PARTICLE MODEL

A. Langevin dynamics for the active bound states

We consider a pair of Brownian particles in the overdamped limit with positions $x_1(t), x_2(t) \in \mathbb{R}$ and diffusivity D_x. Each particle is confined in a harmonic potential with

*These authors contributed equally to this work.
†t.bertrand@imperial.ac.uk

time-dependent stiffness $k_{1,2}(t)$ generated by the other particle. The governing equations then take the form

$$\dot{x}_1 = -k_1(x_1 - x_2) - \partial_{x_1} U_r(|x_1 - x_2|) + \sqrt{2D_x}\xi_1, \quad (1a)$$

$$\dot{x}_2 = -k_2(x_2 - x_1) - \partial_{x_2} U_r(|x_1 - x_2|) + \sqrt{2D_x}\xi_2, \quad (1b)$$

where $\xi_{1,2}(t)$ are uncorrelated zero-mean, unit-variance Gaussian white noises and $U_r(r)$ is a short-range, reciprocal, purely repulsive potential. For the time being, we focus on the case $U_r \equiv 0$, for which a number of closed-form exact results can be derived. We will later show that introducing steric interactions strongly enhances the observed nonequilibrium behavior. We consider binding potential stiffnesses of the form $k_i(t) = \bar{k} + \kappa_i(t)$, where $\bar{k} > 0$ is a constant mean stiffness introduced to ensure that the two particles remain in proximity of each other and $\kappa_{1,2}(t)$ are governed by zero-mean Markov processes setting the stiffness fluctuations [24,30].

Through a change of variables to the center of mass $x = (x_1 + x_2)/2$ and interparticle displacement $y = x_1 - x_2$ coordinates, we can rewrite Eq. (1) as

$$\dot{x}(t) = -\frac{1}{2}\psi(t)y(t) + \sqrt{D_x}\xi_x(t), \quad (2a)$$

$$\dot{y}(t) = -(\varphi(t) + 2\bar{k})y(t) + \sqrt{4D_x}\xi_y(t), \quad (2b)$$

where $\xi_{x,y}(t)$ are again uncorrelated zero-mean unit-variance Gaussian white noise terms (see details in Appendix A). In writing Eq. (2), we have also defined the *stiffness asymmetry* $\psi(t) = \kappa_1(t) - \kappa_2(t)$ and the *total stiffness fluctuations* $\varphi(t) = \kappa_1(t) + \kappa_2(t)$. Note that $\psi(t) \neq 0$ is the signature of *broken reciprocal symmetry* and corresponds to the case where Eq. (2a) for the center of mass can be mapped onto the dynamics of an overdamped active particle with stochastic self-propulsion velocity $v(t) = -\psi(t)y(t)/2$.

While here we focus for simplicity on the one-dimensional case, $x_{1,2} \in \mathbb{R}$, the extension to the more physically relevant case $\mathbf{x}_{1,2} \in \mathbb{R}^3$ is straightforward due to the central nature of the effective forces involved. In particular, it only requires the introduction of an additional degree of freedom describing the orientation $\hat{u}$ of the dimer, which undergoes Brownian motion on the unit sphere ($|\hat{u}| = 1$) with diffusivity $D_u(t) = 2D_x/y(t)^2$ which is only dependent on the magnitude of the interparticle displacement via a change of variables from Cartesian coordinates to spherical polar coordinates.

We study both the dynamics and thermodynamics of these two-particle bound states. To quantify their collective dynamics, we derive exact analytical expressions for the time-dependent mean-square displacement (MSD) of their center of mass, $\langle (x(t) - x(0))^2 \rangle$ [hereafter, setting $x(0) = 0$ by translational symmetry]. From Eq. (2a), this MSD can be expressed in terms of the correlator $\langle \psi(s)\psi(s')y(s)y(s')\rangle$; as shown in Appendix B 1, the decoupling between the dynamics of y and ψ allows us to factorize it, and we write

$$\langle x^2(t)\rangle = D_x t + \frac{1}{4}\int_0^t ds \int_0^t ds' \, \langle \psi(s)\psi(s')\rangle\langle y(s)y(s')\rangle. \quad (3)$$

A long-time effective diffusivity can be extracted by subsequently computing $D_{\text{eff}} = \lim_{t\to\infty}\langle x^2(t)\rangle/(2t)$.

B. Steady-state entropy production rate

The presence of nonreciprocal and fluctuating interactions drives our two-particle bound states out of equilibrium; to quantify this nonequilibrium behavior, we compute the entropy production rate at the level of Eq. (2). We generically expect three contributions, respectively stemming from (i) the dynamics of the center of mass, (ii) the dynamics of the interparticle displacement, and (iii) the stochastic dynamics of the stiffness fluctuations, should they not satisfy detailed balance.

Formally, we write the entropy production rate as the Kullback-Leibler divergence per unit time of the ensemble of forward (x, y, φ, ψ) trajectories and their time-reversed counterparts,

$$\lim_{t\to\infty} \dot{S}_i = \lim_{\tau\to\infty} \frac{1}{\tau}\left\langle \ln \frac{\mathbb{P}_F[x, y, \varphi, \psi]}{\mathbb{P}_R[x, y, \varphi, \psi]}\right\rangle, \quad (4)$$

with $\mathbb{P}_F$ and $\mathbb{P}_R$ denoting corresponding path probability densities, while τ is the path duration. By straightforward manipulation of the joint path probabilities we now write

$$\begin{aligned}\mathbb{P}_{F,R}[x, y, \varphi, \psi] &= \mathbb{P}_{F,R}[y, \varphi, \psi]\mathbb{P}_{F,R}[x|y, \varphi, \psi] \\ &= \mathbb{P}_{F,R}[y, \varphi]\mathbb{P}_{F,R}[\psi|y, \varphi]\mathbb{P}_{F,R}[x|y, \psi], \quad (5)\end{aligned}$$

where in the second equality we have used that x is independent of φ by Eq. (2a). We further assume, as is the case in all models studied here, that ψ is independent of y and φ, whereby $\mathbb{P}_{F,R}[\psi|y, \varphi] = \mathbb{P}_{F,R}[\psi]$. Substituting back into Eq. (4) for the entropy production rate and writing logarithms of products as sums, we arrive by linearity of expectation at

$$\begin{aligned}\lim_{t\to\infty} \dot{S}_i = \lim_{\tau\to\infty} \frac{1}{\tau}\left\langle \ln \frac{\mathbb{P}_F[\psi]}{\mathbb{P}_R[\psi]}\right\rangle + \lim_{\tau\to\infty} \frac{1}{\tau}\left\langle \ln \frac{\mathbb{P}_F[y, \varphi]}{\mathbb{P}_R[y, \varphi]}\right\rangle \\ + \lim_{\tau\to\infty} \frac{1}{\tau}\left\langle \ln \frac{\mathbb{P}_F[x|y, \psi]}{\mathbb{P}_R[x|y, \psi]}\right\rangle. \quad (6)\end{aligned}$$

In all models studied here, we only consider stiffness fluctuations ψ generated by equilibrium processes, satisfying time-reversal symmetry, and thus the first term in the above equation vanishes.

The second term corresponds to the entropy production of the marginal dynamics (y, φ); the dynamics of the interparticle displacement $y(t)$ can be mapped onto those of a single Brownian particle subject to diffusion in a stochastically evolving potential, $U(y, t) = (\varphi(t) + 2\bar{k})y^2/2$, a case which we previously studied in Ref. [24], from which expressions for this term can be read off. This contribution to the entropy production is denoted $\dot{S}_i^{(y)}$.

Finally, the center of mass moves following a drift-diffusion process with a time-dependent drift $v(t) = -\psi(t)y(t)/2$ and diffusivity $D_x/2$; this contribution to the entropy production rate thus takes the form $\lim_{t\to\infty}\dot{S}_i^{(x)} = 2\langle v^2(t)\rangle/D_x$ [31]. To show this, we start from the last term in Eq. (6) and express the conditional path probabilities for the x dynamics as governed by the Langevin equation (2a) in the Onsager-Machlup path integral formalism

$$\mathbb{P}_F[x|y, \psi] \propto \exp\left[-\frac{1}{2D_x}\int_0^\tau dt \left(\dot{x} + \frac{y\psi}{2}\right)^2\right], \quad (7a)$$

$$\mathbb{P}_R[x|y, \psi] \propto \exp\left[-\frac{1}{2D_x}\int_0^\tau dt \left(\dot{x} - \frac{y\psi}{2}\right)^2\right], \quad (7b)$$

where stochastic integrals are to be interpreted in the Stratonovich midpoint convention. Substituting into the last term in Eq. (6), we thus have

$$\lim_{\tau\to\infty}\frac{1}{\tau}\left\langle \ln\frac{\mathbb{P}_F[x|y,\psi]}{\mathbb{P}_R[x|y,\psi]}\right\rangle = -\lim_{\tau\to\infty}\frac{1}{\tau D_x}\int_0^\tau dt\,\langle \dot{x}(t)\psi(t)y(t)\rangle = \frac{\langle\psi^2y^2\rangle}{2D_x}. \tag{8}$$

Using Eq. (8) and the assumption that the ψ dynamics are equilibrium, we conclude from Eq. (6) that the total rate of entropy production can then be written as [24,32]

$$\lim_{t\to\infty}\dot{S}_i = \lim_{t\to\infty}\left(\dot{S}_i^{(x)} + \dot{S}_i^{(y)}\right) = \frac{\langle\psi^2y^2\rangle}{2D_x} + \lim_{t\to\infty}\dot{S}_i^{(y)}. \tag{9}$$

In what follows, we consider two examples of specific prescriptions for the governing stochastic dynamics of the stiffness fluctuations $\kappa_{1,2}(t)$ and show that transiently nonreciprocal pair interactions lead to persistent motion of the center of mass $x(t)$, akin to that of an active particle. For the sake of clarity, we will use in what follows the notation $\bullet^{(\mathrm{cont})}$ and $\bullet^{(\mathrm{disc})}$ to distinguish between the total steady-state entropy production rates and the effective diffusivities calculated for continuous and discrete stiffness fluctuations, respectively.

III. CONTINUOUS FLUCTUATIONS IN THE INTERACTION POTENTIALS

Suppose that the two stiffness fluctuations follow correlated zero-mean Ornstein-Uhlenbeck (OU) processes with rate μ and diffusivity D_κ,

$$\dot{\kappa}_i = -\mu\kappa_i + \sqrt{2D_\kappa}\,\bar{\eta}_i(t), \quad i\in\{1,2\}, \tag{10}$$

where $\bar{\eta}_{1,2}(t)$ are zero-mean white noises satisfying

$$\langle\bar{\eta}_i(t)\bar{\eta}_j(t')\rangle = C_{ij}\delta(t-t'), \quad \text{with } \mathbf{C} = \begin{pmatrix}1 & \theta\\ \theta & 1\end{pmatrix}, \tag{11}$$

where $\mathbf{C}$ is the symmetric covariance matrix and $\theta\in[-1,1]$ quantifies how correlated the stiffness fluctuations are.

The governing equations for the stiffness asymmetry $\psi(t)$ and total stiffness fluctuations $\varphi(t)$ then take the form

$$\dot{\psi}(t) = -\mu\psi(t) + \sqrt{4D_\kappa(1-\theta)}\,\eta_\psi(t), \tag{12a}$$

$$\dot{\varphi}(t) = -\mu\varphi(t) + \sqrt{4D_\kappa(1+\theta)}\,\eta_\varphi(t), \tag{12b}$$

where $\eta_{\psi,\varphi}(t)$ are now *uncorrelated*, zero-mean unit-variance Gaussian white noise terms (see Appendix B). In each of the two limits $\theta=\pm1$, one of the noise terms disappears. For all $\theta>-1$, the interparticle displacement behaves as a Brownian particle in a confining potential with a stiffness that itself follows an Ornstein-Uhlenbeck process with mean $2\bar{k}$ and variance $2D_\kappa(1+\theta)/\mu$.

The dynamics for φ and ψ are independent, which implies that $\langle\psi^2y^2\rangle = \langle\psi^2\rangle\langle y^2\rangle$ factorizes in the second term of Eq. (9). Both contributions to the entropy production rate thus can be written in terms of the variance of the interparticle displacement, assuming that the latter is finite; the first is obtained by the results of Ref. [24], while the second is deduced from the knowledge of the correlator for ψ:

$$\lim_{t\to\infty}\dot{S}_i^{(\mathrm{cont})}(t) = \frac{\bar{k}\mu}{2D_x}\left(\langle y^2\rangle - \frac{D_x}{\bar{k}}\right) + \frac{D_\kappa(1-\theta)}{D_x\mu}\langle y^2\rangle. \tag{13}$$

Again, we note that there is no direct contribution from the switching dynamics as φ and ψ are governed by equilibrium processes. We show in Appendix B 2 that

$$\langle y^2(t)\rangle = 4D_x\int_{-\infty}^t dt'\exp\left[-4\left(\bar{k}-\frac{2D_\kappa(1+\theta)}{\mu^2}\right)(t-t') + \frac{8D_\kappa(1+\theta)}{\mu^3}\left(e^{-\mu(t-t')}-1\right)\right], \tag{14}$$

which remains finite only if $2D_\kappa(1+\theta) < \bar{k}\mu^2$, in which case Eq. (13) can be computed exactly [see Fig. 1(b)]. Consistently with the second law of thermodynamics, $\bar{k}\langle y^2\rangle \geqslant D_x$ [24].

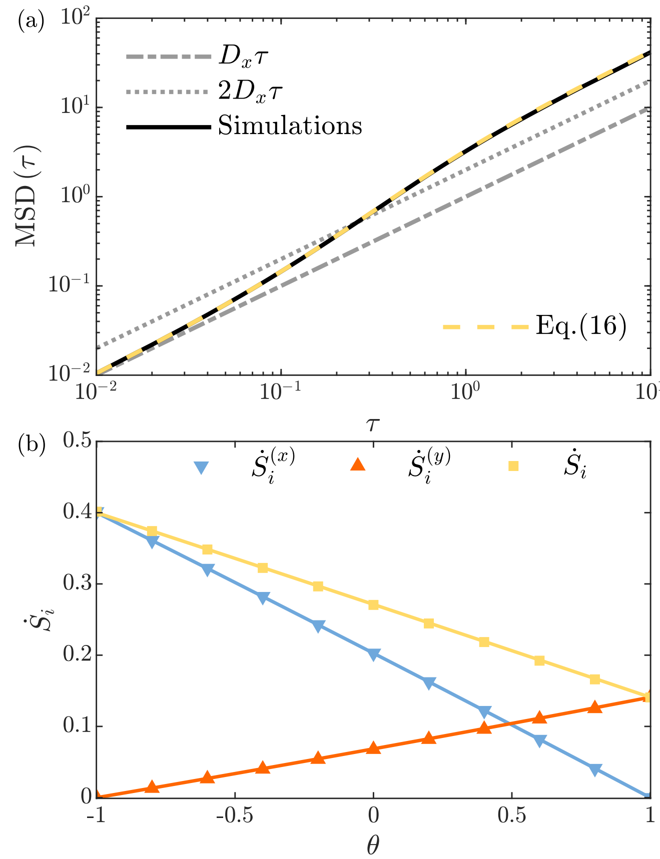

FIG. 1. MSD and entropy production rate for correlated continuous fluctuations. (a) MSD for the active bound states as given by Eq. (16), where we observe transient ballistic scaling implying persistent motion and an effective diffusion coefficient larger than that of an isolated particle. Here, $D_\kappa = 5$ and $D_x = \bar{k} = \mu = 1$. (b) Rate of entropy production for the active bound state, made up of two contributions as identified in Eq. (13), for $\bar{k} = 5$, $D_x = 1$, and $D_\kappa = \mu = 10$. Symbols are from numerical simulations (see Appendix F for details), and solid lines are evaluated using Eqs. (13) and (14).

A. Maximally nonreciprocal fluctuations

We now consider the limit $\theta = -1$, which maximizes how nonreciprocal the interaction fluctuations can be, generating the most interesting joint dynamics. Here, the total stiffness $\varphi(t) \to 0$ in a deterministic manner and the dynamics of both $y(t)$ and $\psi(t)$ reduce to independent, equilibrium diffusive processes in an external potential. The drift term for the center of mass $x(t)$ is the product of these two equilibrium processes [29,33].

The stationary probability distribution for the product $\omega = \psi y$ can be evaluated formally as $P_\omega(\omega) = \int_{-\infty}^{\infty} d\omega' P_\psi(\omega/\omega') P_y(\omega')/|\omega'|$, where P_ψ and P_y denote the Boltzmann steady-state probability densities of the corresponding (equilibrium) processes. We can then derive an expression for the stationary distribution for the drift $P_v(v = -\omega/2)$ through a transformation of probability density functions. It reads

$$P_v\left(v = -\frac{\psi y}{2}\right) = \frac{1}{\pi}\sqrt{\frac{\bar{k}\mu}{D_x D_\kappa}} K_0\left[\sqrt{\frac{\bar{k}\mu}{D_x D_\kappa}}|v|\right] \tag{15}$$

with K_0 being the modified Bessel function of the second kind.

In the present limit, the MSD for the center of mass $x(t)$ is easily calculated as the two-time correlators for $\psi(t)$ and $y(t)$ are those of an equilibrium OU process. Using Eq. (3), we obtain

$$\langle x^2(t)\rangle = D_x t + \frac{2D_\kappa D_x}{\mu\bar{k}(\mu+2\bar{k})^2}\left[e^{-(\mu+2\bar{k})|t|} - 1 + (\mu + 2\bar{k})t\right], \tag{16}$$

which exhibits the *diffusive-ballistic-diffusive* scaling characteristic of active particles [33], as shown in Fig. 1(a). Comparing the form of this MSD to that of a general active particle [33,34], which we derive in Appendix E, we identify an effective self-propulsion speed $v_0 \equiv (D_\kappa D_x/\mu\bar{k})^{1/2}$, persistence time $\tau_p \equiv (\mu + 2\bar{k})^{-1}$, and bare diffusivity $D \equiv D_x/2$. At short timescales, $t \ll \tau_p$, the center of mass follows a diffusive motion with diffusion coefficient D_x. At long times, the dimer exhibits diffusive motion characterized by the long-time effective diffusion coefficient

$$D_{\text{eff}}^{(\text{cont})} = \lim_{t\to\infty} \frac{\langle x^2(t)\rangle}{2t} = \frac{D_x}{2}\left[1 + \frac{2D_\kappa}{\mu\bar{k}(\mu + 2\bar{k})}\right], \tag{17}$$

which is strictly larger than the bare center of mass translational diffusivity, $D_x/2$, when $D_\kappa > 0$, i.e., in the presence of fluctuations. For sufficiently strong fluctuations, specifically $2D_\kappa > \mu\bar{k}(\mu + 2\bar{k})$, this effective diffusivity can strikingly exceed that of a single particle. This is in stark contrast with the classical $1/N$ scaling for the diffusivity of N identical Langevin processes interacting by equilibrium pair interactions and thus represents a genuinely nonequilibrium feature of the present model. Below, we show numerically that this result holds in the presence of repulsive interactions.

To quantify these nonequilibrium dynamics, we evaluate the rate of entropy production from Eq. (13). For $\theta = -1$, we note that the variance of the interparticle displacement satisfies $\langle y^2\rangle = D_x/\bar{k}$, such that the only nonzero contribution to the entropy production rate comes from the center of mass dynamics $x(t)$. Using Eq. (13), we write this as

$$\lim_{t\to\infty} \dot{S}_i^{(\text{cont})}(t)\Big|_{\theta=-1} = \frac{2D_\kappa}{\bar{k}\mu}. \tag{18}$$

This result can also be obtained via the familiar relation $\dot{S}_i = v_0^2/D$ for an active particle [31], with effective self-propulsion speed v_0 and diffusivity D as defined below Eq. (16), highlighting the thermodynamic (as well as dynamic) correspondence between active bound states and active particles. Furthermore, the increase in the effective diffusion coefficient identified in Eq. (17) can be written in terms of the ratio in Eq. (18), confirming that this enhancement is a genuinely nonequilibrium feature of the model.

B. Maximally reciprocal fluctuations

We now briefly discuss the limit $\theta = 1$, in which case the interactions are always reciprocal [since $\psi(t) \to 0$ exponentially after initialization], but the fluctuations in the coupling strength alone are sufficient to drive the system out of equilibrium [24,35,36]. Under these conditions, the center of mass $x(t)$ is diffusive, and its dynamics decouple from that of the interparticle displacement $y(t)$, which itself behaves as a Brownian particle in a fluctuating potential, $U_{\text{tot}}(y, t) = (2\bar{k} + \varphi(t))y^2/2$.

In other words, $y(t)$ is subject to the action of a harmonic confining potential with a stiffness that itself follows an Ornstein-Uhlenbeck process with stiffness μ and mean $2\bar{k}$. The thermodynamics of this model were previously studied in Ref. [24]: The average rate of entropy production has only one nonzero contribution,

$$\lim_{t\to\infty} \dot{S}_i^{(\text{cont})}(t)\Big|_{\theta=1} = \lim_{t\to\infty} \dot{S}_i^{(y)}(t) = \frac{\mu\bar{k}}{2D_x}\left(\langle y^2\rangle - \frac{D_x}{\bar{k}}\right), \tag{19}$$

which can be evaluated using Eq. (14) for the variance of the interparticle displacement. Notably, it vanishes as $D_\kappa \to 0$, i.e., in the absence of fluctuations, while it diverges as $D_\kappa \to \bar{k}\mu^2/4D_\kappa$.

IV. DISCRETE FLUCTUATIONS IN INTERACTION POTENTIALS

We now turn to the case of discrete stiffness fluctuations. We let $\kappa_{1,2}(t) \in \{-\kappa_0, +\kappa_0\}$ be correlated symmetric telegraph processes [37]; the symmetric nature of the Markov jump process ensures that $\langle\kappa_{1,2}(t)\rangle = 0$ and, hence, that pair interactions remain on average reciprocal maintaining the particles in a bound state. The joint probability mass function $\mathbf{P}(t) = (P_{++}(t), P_{+-}(t), P_{--}(t), P_{-+}(t))$ is generically governed by

$$\frac{d}{dt}\mathbf{P} = \mathbf{M} \cdot \mathbf{P}, \tag{20}$$

in which the position-independent Markov matrix $\mathbf{M}$ capturing the stochastic dynamics of the stiffnesses reads

$$\mathbf{M}(\chi) = \lambda[(1 - \chi)\mathbf{M}_{\text{mono}} + \chi\mathbf{M}_{\text{bi}}] \tag{21}$$

with transition rate $\lambda > 0$, correlation parameter $\chi \in [0, 1]$, and transition rate matrices defined as

$$\mathbf{M}_{\text{mono}} = \begin{bmatrix} -2 & 1 & 0 & 1 \\ 1 & -2 & 1 & 0 \\ 0 & 1 & -2 & 1 \\ 1 & 0 & 1 & -2 \end{bmatrix},$$

$$\mathbf{M}_{\text{bi}} = \begin{bmatrix} -1 & 0 & 1 & 0 \\ 0 & -1 & 0 & 1 \\ 1 & 0 & -1 & 0 \\ 0 & 1 & 0 & -1 \end{bmatrix}. \tag{22}$$

The limit $\chi = 0$ leads to bipartite dynamics, where each switching event causes a transition between reciprocal and nonreciprocal interaction. In contrast, $\chi = 1$ corresponds to maximally correlated switching dynamics, such that switching events are always synchronized and the (non)reciprocity of the dynamics is conserved by the fluctuations. While a study of the ensuing dynamics in the general case is of great interest, we consider here the limiting case $\chi = 1$ only, such that $\mathbf{M} = \lambda\mathbf{M}_{\text{bi}}$. In this limit, the fluctuations of φ and ψ are uncorrelated.

A. Maximally nonreciprocal fluctuations

Similarly to what was done for the continuous case, we further focus on the case where fluctuations are maximally nonreciprocal. Let $\kappa_1(0) = -\kappa_2(0) \equiv \kappa_0$ at initialization, such that $|\psi(t)| = 2\kappa_0$ and $\varphi(t) = 0$. The synchrony condition $\chi = 1$ imposes that the total stiffness $\varphi(t)$ remains zero while the sign of the stiffness asymmetry $\psi(t)$ switches with symmetric Poisson rate λ, a telegraph process, leading to nonreciprocal force fluctuations at all times (see details of allowed transitions for the Markov jump process in Appendix C). The dynamics of $y(t)$ are exactly those of a diffusive particle in the potential $U(y) = \bar{k}y^2$. We note that $\langle\psi(s)\psi(s')\rangle = 4\kappa_0^2 e^{-2\lambda|s-s'|}$, while $\langle y(s)y(s')\rangle = (D_x/\bar{k})e^{-2\bar{k}|s-s'|}$ is simply the propagator for an Ornstein-Uhlenbeck process [37]. As shown in Appendix C, we conclude that the full MSD then takes the form

$$\langle x^2(t)\rangle = D_x t + \frac{D_x\kappa_0^2}{2\bar{k}(\lambda+\bar{k})^2}\left[e^{-2(\lambda+\bar{k})t} - 1 + 2(\lambda+\bar{k})t\right] \tag{23}$$

[see Fig. 2(a)], which again can be mapped to the MSD of an active particle with effective self-propulsion speed $v_0 \equiv \kappa_0(D_x/\bar{k})^{1/2}$, persistence time $\tau_p \equiv (2(\lambda+\bar{k}))^{-1}$, and bare diffusivity $D \equiv D_x/2$ [33,34]. Finally, the long-time effective diffusion coefficient reads

$$D_{\text{eff}}^{(\text{disc})} = \frac{D_x}{2}\left(1 + \frac{\kappa_0^2}{\bar{k}(\lambda+\bar{k})}\right), \tag{24}$$

which is strictly larger than the bare center of mass translational diffusivity. Remarkably, for sufficiently slow fluctuations, specifically $\lambda < \bar{k}(\kappa_0^2/\bar{k}^2 - 1)$, this effective diffusivity can exceed that of a single particle as we saw for the case of continuous fluctuations [see Fig. 2(a)].

As the dynamics for $y(t)$ is at equilibrium, the only nonzero contribution to the entropy production comes from the spontaneous drift of the center of mass. In the present case, the dynamics of $\psi(t)$ and $y(t)$ are again entirely decoupled implying that $\langle\psi^2 y^2\rangle = \langle\psi^2\rangle\langle y^2\rangle$. We can evaluate $\langle\psi^2\rangle = 4\kappa_0^2$, $\langle y^2\rangle = D_x/\bar{k}$ [37] and using Eq. (9) write the full entropy production rate as

$$\lim_{t\to\infty} \dot{S}_i^{(\text{disc})}(t) = \frac{2\kappa_0^2}{\bar{k}}. \tag{25}$$

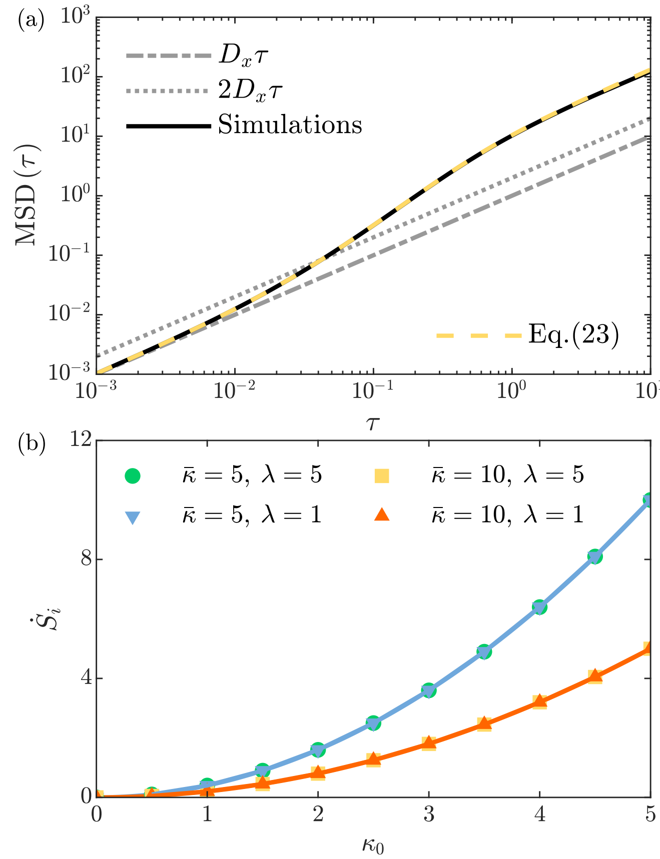

FIG. 2. MSD and entropy production rate for synchronized discrete fluctuations. (a) MSD for the active bound states as given by Eq. (23) again displaying transient ballistic scaling and enhanced diffusion. Here, $\kappa_0 = 5$ and $D_x = \bar{k} = \lambda = 1$. (b) Rate of entropy production for the active bound state where we have fixed $D_x = 1$. Symbols are measured from numerical simulations, and solid lines are the results of Eq. (25).

The independence of Eq. (25) from the switching rate λ is demonstrated numerically in Fig. 2(b). Similarly to Eq. (18), this result can also be obtained by direct substitution of the effective self-propulsion speed v_0 and bare diffusivity D as defined below Eq. (23) into the familiar formula for the entropy production of an active particle $\dot{S}_i = v_0^2/D$ [31]. As for the continuous fluctuations above, the rescaled effective diffusion coefficient can be written in terms of this entropy production rate. This shows that our mapping to active bound states can be done at the level of the dynamics (mean-square displacement) or thermodynamics (entropy production rate).

B. Maximally reciprocal fluctuations

We now briefly discuss the case of fluctuating reciprocal couplings, whereby we let $\kappa_1(0) = \kappa_2(0) = \kappa_0$ at initialization. This choice of initial condition leads to a vanishing stiffness asymmetry $\psi(t) = 0$ at all times, while the total stiffness $\varphi(t) \in \{-2\kappa_0, 2\kappa_0\}$ is now governed by a telegraph process with Poisson switching rate λ. The center of mass dynamics are here purely diffusive with $\dot{x}(t) = \sqrt{D_x}\xi_x$, leading trivially to a MSD $\langle x^2(t)\rangle = D_x t$, whereas the displacement dynamics are identical to those of a Brownian particle in an intermittent harmonic potential $U_{\mathrm{tot}}(y, \varphi) = (2\bar{k} + \varphi(t))y^2/2$. Existence of the second moment of the interparticle displacement requires $\kappa_0^2 < \bar{k}^2 + \lambda\bar{k}/2$ [35,36].

To obtain an explicit form for the entropy production in this case, we can use the result of Ref. [24], whence

$$\lim_{t\to\infty} \dot{S}_i^{(\mathrm{disc})}(t) = \frac{2\kappa_0^2\lambda}{2(\bar{k}^2 - \kappa_0^2) + \lambda\bar{k}}, \tag{26}$$

which vanishes as $\kappa_0 \to 0$ and diverges as $\kappa_0 \to \sqrt{\bar{k}^2 + \lambda\bar{k}/2}$.

V. EFFECT OF STERIC REPULSION

So far, we have ignored the role of steric repulsion; while this allowed us to derive exact analytical results, we now reintroduce a nonvanishing purely repulsive potential $U_r \neq 0$ in Eq. (1). While the equation governing the center of mass dynamics is unaffected by this change, Eq. (2b) for the interparticle displacement acquires an additional term

$$\dot{y}(t) = -(\varphi(t) + 2\bar{k})y(t) - 2\partial_y U_r(y) + \sqrt{4D_x}\xi_y(t). \tag{27}$$

Intuitively, since U_r should penalize particles overlapping, we expect the bound state to be characterized by a finite interparticle displacement, commensurate with the particle diameter. If we further assume that the fluctuations in y are small, then $y(t) \approx \sqrt{\langle y^2\rangle}$ is approximately constant and $\psi(t)$ is left to be the sole term responsible for fluctuations in the self-propulsion contribution to the center of mass dynamics in Eq. (2a). Remarkably, when $\psi(t)$ is an OU process, such as in Eq. (12b), the ensuing dynamics of the bound state are then akin to those of an *active Ornstein-Uhlenbeck* particle (AOUP). Similarly, when $\psi(t)$ is governed by a telegraph process, which is exactly the case which leads to Eq. (23), the dynamics match those of a *run-and-tumble* particle (RTP).

To study numerically the effect that steric repulsion has on our results, we choose a Weeks-Chandler-Anderson potential for $U_r(r)$, capped at $r_c = 2^{1/6}$ to give the particles a well-defined diameter (see Refs. [38,39] and Appendix F). Strikingly, the MSDs exhibit a significantly increased long-time diffusion coefficient for the case of nonreciprocal fluctuations, as can be seen in Fig. 3. The average rate of entropy production remains qualitatively unchanged by the introduction of steric repulsion showing the characteristic monotonic increase already seen in Fig. 2 (see Appendix D), albeit at an overall level which is is approximately one order of magnitude higher. We rationalize this by arguing that, by keeping the two particles apart, repulsion leads to much larger average forces coming from the harmonic potential, driving more persistent motion and hence higher dissipation in the present model.

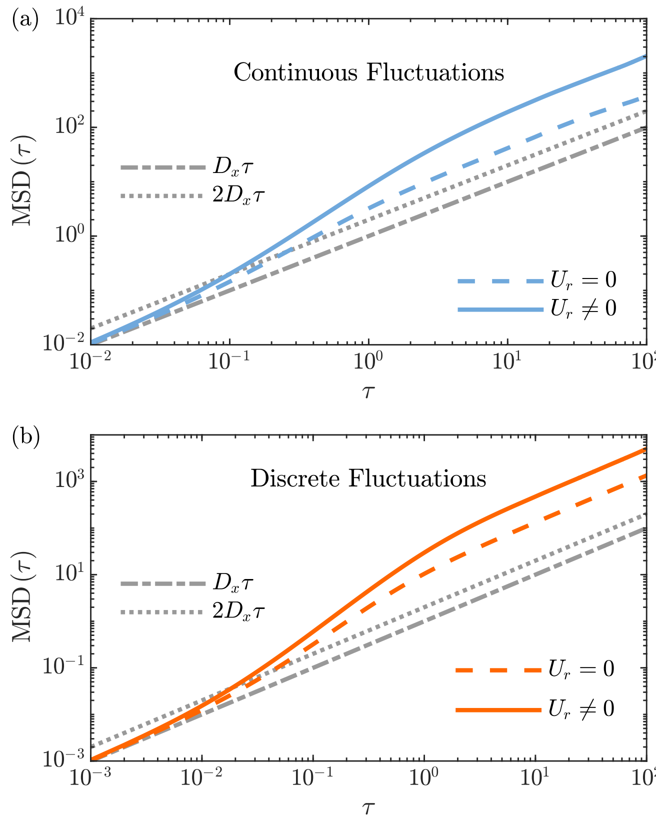

FIG. 3. Steric repulsion enhances persistent motion. We compare our results on the dimer's dynamics above to simulations which include a repulsive force between the two particles through a Weeks-Chandler-Anderson potential. For both (a) continuous and (b) discrete fluctuations, this additional interaction leads to a significantly enhanced effective diffusion coefficient. Parameters are the same as in Figs. 1(a) and 2(a).

VI. DISCUSSION AND CONCLUSION

We have demonstrated that reciprocal-symmetry-breaking fluctuations about a reciprocal mean attractive coupling are sufficient to generate two-particle bound states whose center of mass motion can be mapped onto that of a motile active particle, Eq. (2a). For specific choices of the fluctuations and in the presence of steric repulsion, one-dimensional *active Ornstein-Uhlenbeck* as well as *run-and-tumble* dynamics are approximately recapitulated. We characterize the dissipative nature of these active bound states by computing the average rate of entropy production, Eq. (9). Remarkably, for sufficiently strong nonreciprocal fluctuations, the long-time effective diffusion is observed to exceed that of a single particle, Eqs. (17) and (24), which represents a genuinely nonequilibrium feature of our model.

Fluctuations in the degree of reciprocity of pair interactions arise naturally in a number of physical circumstances, e.g., through mediation by a nonequilibrium medium [4–8], in the presence of memory [10], or from perception within a finite vision cone [18,40]. In fact, in macroscopic active systems, nonreciprocity is arguably the norm rather than the exception.

Fluctuating nonreciprocal interactions have been realized in two-body systems in recent studies on nanoparticles [20] and magnetic microdisks [21] subjected to random and oscillating external fields, respectively. In both cases, the resulting pair interactions lead to persistent motion as predicted in the theory above. Another promising candidate for realizing the dynamics studied here could be size-dependent interactions between droplets exchanging mass through inverse Ostwald ripening dynamics [3]. In general, the strength of interactions through a medium depends on the perimeter of a droplet, which is a dynamic quantity due to thermal fluctuations driving constant rebalancing of the Laplace pressure.

ACKNOWLEDGMENTS

L.C. acknowledges support from the Francis Crick Institute, which receives its core funding from Cancer Research UK, the UK Medical Research Council, and the Wellcome Trust (FC001317). H.A. was supported by a Roth Ph.D. scholarship funded by the Department of Mathematics at Imperial College London.

APPENDIX A: CHANGE OF FRAME OF REFERENCE

It is instructive to consider the dynamics of this two-particle system in an alternative frame of reference by defining the center of mass $x = (x_1 + x_2)/2$ and interparticle displacement $y = x_1 - x_2$ coordinates. From Eq. (1), we can derive governing equations for the dynamics of these two variables:

$$\dot{x}(t) = -\tfrac{1}{2}(\kappa_1 - \kappa_2)y(t) + \sqrt{D_x/2}(\xi_1(t) + \xi_2(t)), \quad \text{(A1a)}$$

$$\dot{y}(t) = -(\kappa_1 + \kappa_2 + 2\bar{k})y(t) + \sqrt{2D_x}(\xi_1(t) - \xi_2(t)). \quad \text{(A1b)}$$

The noise terms can be rewritten succinctly each as a single Gaussian white noise term. Indeed, we define the noise terms

$$\xi_x(t) = \tfrac{1}{2}(\xi_1(t) + \xi_2(t)), \quad \text{(A2a)}$$

$$\xi_y(t) = \tfrac{1}{2}(\xi_1(t) - \xi_2(t)), \quad \text{(A2b)}$$

where we include the prefactors of $1/2$ such that both ξ_x and ξ_y have zero mean and unit variance, while also remaining independent:

$$\langle \xi_x(t) \rangle = \tfrac{1}{2}(\langle \xi_1(t) \rangle + \langle \xi_2(t) \rangle) = 0, \quad \text{(A3a)}$$

$$\langle \xi_y(t) \rangle = \tfrac{1}{2}(\langle \xi_1(t) \rangle - \langle \xi_2(t) \rangle) = 0, \quad \text{(A3b)}$$

$$\begin{aligned}\langle \xi_x(t)\xi_x(t') \rangle &= \tfrac{1}{2}(\langle \xi_1(t)\xi_1(t') \rangle + \langle \xi_2(t)\xi_2(t') \rangle)\\ &= \delta(t - t'), \quad \text{(A3c)}\end{aligned}$$

$$\begin{aligned}\langle \xi_y(t)\xi_y(t') \rangle &= \tfrac{1}{2}(\langle \xi_1(t)\xi_1(t') \rangle + \langle \xi_2(t)\xi_2(t') \rangle)\\ &= \delta(t - t'). \quad \text{(A3d)}\end{aligned}$$

We define the *stiffness asymmetry* $\psi(t) = \kappa_1(t) - \kappa_2(t)$ and the *total stiffness fluctuations* $\varphi(t) = \kappa_1(t) + \kappa_2(t)$, where we remark that $\psi(t) \neq 0$ is the signature of *broken reciprocal symmetry* at time t.

In all, this leads us to rewriting Eq. (1) in the new frame of reference as

$$\dot{x}(t) = -\tfrac{1}{2}\psi(t)y(t) + \sqrt{D_x}\xi_x(t), \quad \text{(A4a)}$$

$$\dot{y}(t) = -(\varphi(t) + 2\bar{k})y(t) + \sqrt{4D_x}\xi_y(t). \quad \text{(A4b)}$$

APPENDIX B: CONTINUOUS STIFFNESS FLUCTUATIONS

1. Full derivation of the time-dependent MSD

In this Appendix, we give the full derivation for the MSD for the case where the spatial dynamics are given by Eqs. (2) and the stiffness fluctuations $\kappa_i(t)$ are correlated Ornstein-Uhlenbeck processes with rate μ and diffusivity D_κ,

$$\dot{\kappa}_i(t) = -\mu\kappa_i(t) + \sqrt{2D_\kappa}\bar{\eta}_i(t), \quad i \in \{1, 2\}, \quad \text{(B1)}$$

with $\bar{\eta}_{1,2}(t)$ taken to be zero-mean white noises satisfying

$$\langle \bar{\eta}_i(t)\bar{\eta}_j(t') \rangle = C_{ij}\delta(t - t'), \quad \text{with } \mathbf{C} = \begin{pmatrix} 1 & \theta \\ \theta & 1 \end{pmatrix}. \quad \text{(B2)}$$

As above, $\mathbf{C}$ denotes the symmetric covariance, and $\theta \in [-1, 1]$ quantifies how correlated the stiffness fluctuations are. The stiffness asymmetry $\psi(t) = \kappa_1(t) - \kappa_2(t)$ and the total stiffness fluctuations $\varphi(t) = \kappa_1(t) + \kappa_2(t)$ are then governed by

$$\dot{\psi}(t) = -\mu\psi(t) + \sqrt{4D_\kappa(1 - \theta)}\eta_\psi(t), \quad \text{(B3a)}$$

$$\dot{\varphi}(t) = -\mu\varphi(t) + \sqrt{4D_\kappa(1 + \theta)}\eta_\varphi(t) \quad \text{(B3b)}$$

with $\langle \eta_i(t)\eta_j(t') \rangle = \delta_{ij}\delta(t - t')$.

Consider the dynamics for y in the limit where $\theta = -1$. The governing equations take the form

$$\dot{x}(t) = -\psi(t)y(t)/2 + \sqrt{D_x}\xi_x(t), \quad \text{(B4a)}$$

$$\dot{y}(t) = -2\bar{k}y(t) + \sqrt{4D_x}\xi_y(t), \quad \text{(B4b)}$$

$$\dot{\psi}(t) = -\mu\psi(t) + \sqrt{8D_\kappa}\eta_\psi(t) \quad \text{(B4c)}$$

with $\varphi(t) = 0$ provided the right initial conditions. Integrating in time, we derive the solution

$$y(t) = y_0 e^{-2\bar{k}t} + \sqrt{4D_x}\int_0^t ds\, \xi_y(s)e^{-2\bar{k}(t-s)}. \quad \text{(B5)}$$

Taking an average over the noise, we see that $\langle y(t) \rangle = y_0 e^{-2\bar{k}t}$. To evaluate the mean-square displacement of the center of mass, $\langle (x(t) - x_0)^2 \rangle$, we set $x_0 = 0$ and write

$$\begin{aligned}\langle x^2(t) \rangle = \bigg\langle &\int_0^t ds\bigg(-\frac{1}{2}\psi(s)y(s) + \sqrt{D_x}\xi_x(s)\bigg)\\ &\times \int_0^t ds'\bigg(-\frac{1}{2}\psi(s')y(s') + \sqrt{D_x}\xi_x(s')\bigg)\bigg\rangle\end{aligned}$$

leading to

$$\langle x^2(t) \rangle = \int_0^t ds \int_0^t ds' \frac{1}{4}\langle \psi(s)\psi(s')y(s)y(s') \rangle + D_x\delta(s - s'). \quad \text{(B6)}$$

As y and ψ are independent, we can write $\langle \psi(s)\psi(s')y(s)y(s') \rangle = \langle \psi(s)\psi(s') \rangle\langle y(s)y(s') \rangle$. We are thus left with computing the two correlators.

Next, we derive an analytic expression for the time-correlation function $\langle y(t)y(t') \rangle$, working at steady state. To do this, we set $t' > t$ and consider a second correlation function

$$C_y(t, t') = \Big\langle (y(t) - \langle y(t) \rangle)(y(t') - \langle y(t') \rangle) \Big\rangle, \quad \text{(B7)}$$

which we can write as

$$C_y(t, t') = 4D_x\bigg\langle \int_0^t ds\xi_y(s)e^{-2\bar{k}(t-s)} \int_0^{t'} ds'\xi_y(s')e^{-2\bar{k}(t'-s')} \bigg\rangle$$

leading to

$$C_y(t,t') = 4D_x \int_0^t ds \int_0^{t'} ds' e^{-2\bar{k}(t+t'-s-s')} \langle \xi_y(s)\xi_y(s')\rangle = \frac{D_x}{\bar{k}}\left[e^{-2\bar{k}(t'-t)} - e^{-2\bar{k}(t+t')}\right]. \tag{B8}$$

From Eqs. (B7) and (B8), we obtain an analytic expression for the time-correlation function $\langle y(t)y(t')\rangle$ as desired:

$$\langle y(t)y(t')\rangle = \left[y_0^2 - \frac{D_x}{\bar{k}}\right]e^{-2\bar{k}(t+t')} + \frac{D_x}{\bar{k}}e^{-2\bar{k}|t-t'|}, \tag{B9}$$

where we have relaxed the condition that $t' > t$. Following the same procedure, we also derive an expression for $\langle\psi(t)\psi(t')\rangle$:

$$\langle\psi(t)\psi(t')\rangle = \left[\psi_0^2 - \frac{4D_\kappa}{\mu}\right]e^{-\mu(t+t')} + \frac{4D_\kappa}{\mu}e^{-\mu|t-t'|}. \tag{B10}$$

Given these two correlators, we can now obtain an exact expression for the MSD of the center of mass of the dimer

$$\langle x^2(t)\rangle = D_x t + \frac{2D_\kappa D_x}{\mu\bar{k}(\mu+2\bar{k})^2}\left[(\mu+2\bar{k})t + e^{-(\mu+2\bar{k})t} - 1\right]. \tag{B11}$$

Finally, we conclude that the effective diffusion coefficient reads

$$D_{\text{eff}}^{(\text{cont})} = \lim_{t\to\infty}\frac{\langle x^2(t)\rangle}{2t} = \frac{D_x}{2}\left[1 + \frac{2D_\kappa}{\mu\bar{k}(\mu+2\bar{k})}\right]. \tag{B12}$$

2. Variance in particle position for an OU^2

The position y of an overdamped Brownian particle trapped in a harmonic potential whose stiffness fluctuates about its mean value $2\bar{k} > 0$ in the manner of a Ornstein-Uhlenbeck (OU) process is governed by the following stochastic process:

$$\partial_t y(t) = -(2\bar{k} + \varphi(t))y(t) + \sqrt{4D_x}\eta_y(t), \tag{B13a}$$

$$\partial_t \varphi(t) = -\mu\varphi(t) + \sqrt{4(1+\theta)D_\kappa}\eta_\varphi(t), \tag{B13b}$$

where the additive noises satisfy $\langle\eta_i(t)\eta_j(t')\rangle = \delta_{ij}\delta(t-t')$. We dub this stochastic process the OU^2 *process*.

The formal solution for y is given by

$$y(t) = \sqrt{4D_x}\int_{-\infty}^t dt'\ \eta_y(t')e^{-2\bar{k}(t-t') - \int_{t'}^t dt''\varphi(t'')}. \tag{B14}$$

We square this equation and then average over noise realizations to obtain an expression for the variance:

$$\langle y^2(t)\rangle = 4D_x \int_{-\infty}^t dt' \int_{-\infty}^t d\tau' e^{-2\bar{k}(t-t')-2\bar{k}(t-\tau')} \times\left\langle \eta_y(t')\eta_y(\tau')\, e^{-\int_{t'}^t dt''\varphi(t'') - \int_{\tau'}^t d\tau''\varphi(\tau'')}\right\rangle,$$

which leads to

$$\langle y^2(t)\rangle = 4D_x \int_{-\infty}^t dt'\ e^{-4\bar{k}(t-t')}\left\langle e^{-2\int_{t'}^t dt''\varphi(t'')}\right\rangle, \tag{B15}$$

where we used that

$$\left\langle \eta_y(t')\eta_y(\tau')\, e^{-\int_{t'}^t dt''\varphi(t'') - \int_{\tau'}^t d\tau''\varphi(\tau'')}\right\rangle = \delta(t'-\tau')\left\langle e^{-\int_{t'}^t dt''\ \varphi(t'') - \int_{\tau'}^t d\tau''\ \varphi(\tau'')}\right\rangle$$

since η and φ are uncorrelated and thus the expectation factorizes. We now use a standard identity between the moment generating function of the random variable $-2\int_{t'}^t dt''\ \varphi(t'')$ and the exponential of the corresponding cumulant generating function, which in this case gives

$$\left\langle \exp\left[-2\int_{t'}^t dt''\varphi(t'')\right]\right\rangle = \exp\sum_{m=1}^{\infty}\frac{1}{m!}\left\langle\left(-2\int_{t'}^t dt''\ \varphi(t'')\right)^m\right\rangle_c, \tag{B16}$$

where $\langle\cdot\rangle_c$ denotes a cumulant or connected correlation. Since $\varphi(t)$ is a zero-mean OU process, at steady state all cumulants except the second vanish. The latter reads

$$\langle\varphi(t_1)\varphi(t_2)\rangle_c = \frac{8(1+\theta)D_\kappa}{\mu}e^{-\mu|t_1-t_2|}. \tag{B17}$$

Thus

$$\left\langle \exp\left[-2\int_{t'}^t dt''\varphi(t'')\right]\right\rangle = \exp\left(\frac{8(1+\theta)D_\kappa}{\mu}\int_{t'}^t dt''\int_{t'}^t d\tau'' e^{-\mu|t''-\tau''|}\right)$$
$$= \exp\left(\frac{8(1+\theta)D_\kappa}{\mu}\frac{1}{\mu^2}(\mu(t-t') - 1 + e^{-\mu(t-t')})\right)$$
$$= \exp\left(\frac{8(1+\theta)D_\kappa}{\mu^2}(t-t')\right)\exp\left(\frac{8(1+\theta)D_\kappa}{\mu^3}(-1 + e^{-\mu(t-t')})\right). \tag{B18}$$

Going back to Eq. (B15), our expression for the variance reduces to

$$\langle y^2(t)\rangle = 4D_x \exp\left[-\frac{8(1+\theta)D_\kappa}{\mu^3}\right]\int_{-\infty}^t dt'\ \exp\left[-\left(4\bar{k} - \frac{8(1+\theta)D_\kappa}{\mu^2}\right)(t-t')\right]\exp\left[\frac{8(1+\theta)D_\kappa}{\mu^3}e^{-\mu(t-t')}\right], \tag{B19}$$

which constitutes the key result of this section. The integral in the expression above has a divergent contribution as $t' \to -\infty$ when the exponent of the first term in the integrand changes sign. In other words, a necessary and sufficient con-

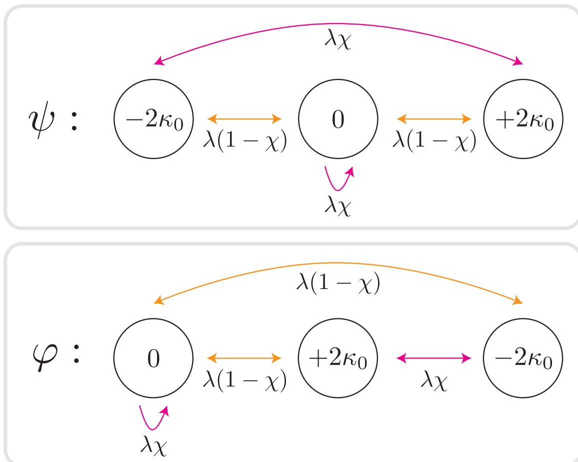

FIG. 4. Allowed transitions for the Markov jump process controlling the stiffness asymmetry $\psi(t)$ and total stiffness fluctuation $\varphi(t)$ in the case of discrete fluctuations in the coupling strength. Here, λ denotes the switching rate, while $\chi \in [0, 1]$ is a correlation parameter controlling the degree of synchronization of the single potential switching events.

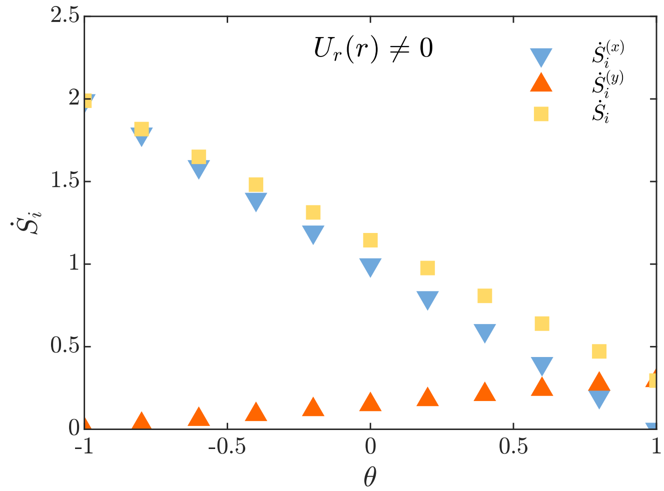

FIG. 5. Entropy production rate when $U_r \neq 0$ for continuous fluctuations. We here use a repulsive potential of Weeks-Chandler-Anderson form. While the functional dependence on the correlation coefficient θ remains similar, the magnitude of all contributions is significantly larger. This agrees with the more persistent motion that we observe in Fig. 3 in the main text.

dition for the existence of the second moment $[\langle y^2(t)\rangle < \infty]$ is

$$\bar{k} > \frac{2(1+\theta)D_\kappa}{\mu^2}. \tag{B20}$$

The main result Eq. (B19) can be integrated numerically to obtain the steady-state variance (in the limit $t \to \infty$) and hence the average rate of entropy production in the two-particle system.

APPENDIX C: FULL DERIVATION OF THE TIME-DEPENDENT MSD FOR DISCRETE STIFFNESS FLUCTUATIONS

Here, we give a full derivation of the time-dependent MSD calculated for the case of synchronized ($\chi = 1$) discrete fluctuations in the main text. The accessible transitions for the Markov processes governing the fluctuations of φ and ψ are shown in Fig. 4. We know that the MSD takes the same general form in the two-particle minimal model considered:

$$\langle x^2(t)\rangle = D_x t + \frac{1}{4}\int_0^t ds \int_0^t ds' \, \langle\psi(s)\psi(s')\rangle\langle y(s)y(s')\rangle. \tag{C1}$$

Therefore we are required to derive expressions for the two correlators. The stiffness asymmetry $\psi(t)$ is a telegraph process acting on $\{-2\kappa_0, 2\kappa_0\}$; thus we can write the correlator as

$$\langle\psi(s)\psi(s')\rangle = \langle\psi^2\rangle e^{-2\lambda|s'-s|} = 4\kappa_0^2 e^{-2\lambda|s'-s|}, \tag{C2}$$

where $\langle\psi^2\rangle = 4\kappa_0^2$ is the variance of ψ. In the absence of a repulsive potential, $U_r = 0$, the dynamics for $y(t)$ are governed by an (equilibrium) Ornstein-Uhlenbeck process, and using Eq. (B9), we write the MSD as

$$\langle x^2(t)\rangle = D_x t + \frac{D_x\kappa_0^2}{\bar{k}}\int_0^t ds \int_0^t ds' e^{-2(\lambda+\bar{k})|s'-s|}. \tag{C3}$$

Finally, we use the fact that, for any constant $A_0 > 0$,

$$\int_0^t ds \int_0^t ds' e^{-A_0|s'-s|} = \frac{2}{A_0^2}\left[A_0 t + e^{-A_0|t|} - 1\right] \tag{C4}$$

to derive the final result

$$\langle x^2(t)\rangle = D_x t + \frac{D_x\kappa_0^2}{2\bar{k}(\lambda+\bar{k})^2}\left[2(\lambda+\bar{k})t + e^{-2(\lambda+\bar{k})|t|} - 1\right], \tag{C5}$$

which satisfies the usual *diffusive-ballistic-diffusive* scaling observed with active particles. Indeed, at very short timescales, $t \ll (2(\lambda+\bar{k}))^{-1}$, the center of mass follows a diffusive motion with diffusion coefficient $D_x/2$. When $t \approx (2(\lambda+\bar{k}))^{-1}$, the two-particle system displays *ballistic* motion, with $\langle x^2(t)\rangle = D_x t + (D_x k_0^2/\bar{k})t^2$ and hence $\langle x^2(t)\rangle \propto t^2$. At large times, the effective diffusion coefficient reads

$$D_{\text{eff}}^{(\text{disc})} = \frac{D_x}{2}\left(1 + \frac{\kappa_0^2}{\bar{k}(\lambda+\bar{k})}\right). \tag{C6}$$

APPENDIX D: EFFECT OF A REPULSIVE POTENTIAL ON THE RATE OF ENTROPY PRODUCTION

In this Appendix, we present numerical results for the entropy production rate in the two-particle system for the case where a repulsive potential is present between the two particles. We have defined the repulsive potential to be of Weeks-Chandler-Anderson form:

$$U_r(r) = \begin{cases} 4\varepsilon[(\sigma/r)^{12} - (\sigma/r)^6] + \epsilon, & r < r_c \\ 0, & r \geqslant r_c \end{cases} \tag{D1}$$

with $r_c = 2^{1/6}\sigma$, to give the particles a well-defined diameter. For the sake of simplicity, we here set $\varepsilon = 1/48$ and $\sigma = 1$.

In Fig. 5, we see the effect for the continuous fluctuations. The linear scaling of the two contributions with the correlation coefficient θ persists, but the overall level of entropy production is approximately one order of magnitude higher. We argue

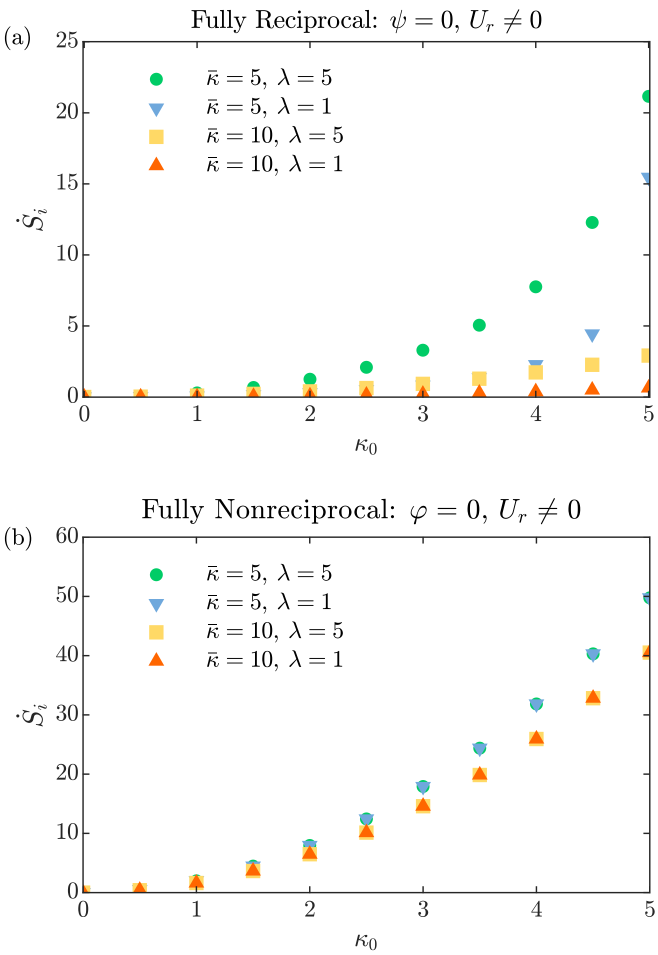

FIG. 6. Entropy production rate when $U_r \neq 0$ for discrete fluctuations. (a) For an initialization which sets $\psi = 0$ in the presence of nonzero U_r. We observe a similar functional dependence on the fluctuation strength κ_0 as in Fig. 2, but the overall amount of entropy produced is significantly larger, as was observed in the continuous case. In (b), the same trend is observed for the initialization which sets $\varphi = 0$.

that this is because the particle separation that is enforced by U_r leads to greater forces stemming from the contribution of the harmonic potentials. These larger forces inevitably lead to the potentials performing more nonequilibrium work, thus enhancing the entropy production.

In Fig. 6, we study the case of discrete fluctuations and observe a similar trend. Notably, the entropy production rate is independent of the switching rate λ for $\varphi = 0$ as in the case $U_r = 0$ (see Fig. 2). This is due to the fact that the dissipation only depends on the square of the velocity, and so the sign switch, which is controlled by λ, does not factor in. The same is observed for a classic one-dimensional, symmetric *run-and-tumble* particle, where the entropy production rate is independent of the Poissonian tumbling rate [31].

APPENDIX E: COMPARISON OF RESULTS TO MSDs OF A GENERIC ACTIVE PARTICLE

Here we rederive a classic result for the mean-square displacement (MSD) of a generic self-propelling particle in one dimension (1D) and then compare the structure of the full expression with the corresponding analytic forms derived for the two examples in the main text.

Consider a self-propelled particle in 1D with the equation of motion

$$\dot{x} = v(t) + \sqrt{2D_x}\eta(t), \tag{E1}$$

where $\eta(t)$ is a zero-mean, unit-variance Gaussian white noise term and $v(t)$ is a generic self-propulsion force. The MSD of the particle position can then be derived as

$$\begin{aligned}\langle x^2(t)\rangle &= \left\langle\left(\int_0^t ds[v(s) + \sqrt{2D}\eta(s)]\right)\right.\\ &\quad\times\left.\left(\int_0^t ds'[v(s') + \sqrt{2D}\eta(s')]\right)\right\rangle\\ &= \int_0^t ds\int_0^t ds'\langle v(s)v(s')\rangle + 2D\delta(s-s').\end{aligned} \tag{E2}$$

To evaluate the leftover integrals, we require an analytic form for the time correlation of the self-propulsion velocity. To make progress, we assume that the governing process for the self-propulsion force is time-translation invariant and that the decay of the correlation function is given or well approximated by an exponential, taking the form

$$\langle v(s)v(s')\rangle = v_0^2 e^{-|s-s'|/\tau_p}, \tag{E3}$$

where we have defined the typical self-propulsion speed as

$$v_0 = \sqrt{\langle v^2(s)\rangle} \tag{E4}$$

(which is independent of s) and τ_p is the persistence time. We note that this form for the correlator is exact for both AOUP and RTP dynamics, where the governing processes for the self-propulsion force are Ornstein-Uhlenbeck and telegraph processes, respectively. It would also capture the dynamics of an active Brownian particle if we were working in higher dimensions (so the diffusion of the self-propulsion direction could be suitable defined). After substituting this expression for the correlator, we evaluate the integrals to derive the following result for the time-dependent MSD of a self-propelling particle:

$$\mathrm{MSD}(\tau) = 2D\tau + 2v_0^2\tau_p^2\left[\frac{\tau}{\tau_p} + e^{-\tau/\tau_p} - 1\right], \tag{E5}$$

with characteristic speed v_0, persistence time τ_p, and bare diffusivity D [33,34].

We use this general form to identify these three features of our active bound state dynamics. In the case of continuous stiffness fluctuations, we identify an effective self-propulsion speed $v_0 = (D_\kappa D_x/\mu\bar{k})^{1/2}$, persistence time $\tau_p = (\mu + 2\bar{k})^{-1}$, and bare diffusivity $D_x/2$. For the case of discrete fluctuations, we identify the characteristic self-propulsion speed $v_0 \equiv \kappa_0(D_x/\bar{k})^{1/2}$, persistence time $\tau_p \equiv (2(\lambda + \bar{k}))^{-1}$, and bare diffusivity $D \equiv D_x/2$.

APPENDIX F: DETAILS OF THE NUMERICAL ANALYSIS

We simulate the Langevin equations in the center-of-mass–interparticle-displacement frame of reference using a stochastic Runge-Kutta method in 1D [39]. We run the solver for different random number seeds for 10^3 time units, only recording data after the first 20% of the simulations so as to let the dynamics reach a steady state.

We measure the entropy production along each trajectory by calculating the heat dissipated at each step in the dynamics of the center of mass $x(t)$ and the interparticle displacement $y(t)$. This is given by the change in the variable multiplied by the effective (deterministic) force exerted on the variable at each time step, evaluated in the Stratonovich convention for stochastic dynamics. For $x(t)$, the force is exactly the drift term identified in the main text: $v(t) = -\psi(t)y(t)/2$. Between t and $t + dt$, we employ the Stratonovich convention for time discretization [31], which implies that the heat dissipated δQ is calculated as

$$\delta Q([t, t+dt)) = \frac{v(t) + v(t+dt)}{2}[x(t+dt) - x(t)]. \quad \text{(F1)}$$

We sum together all the contributions to measure the total heat dissipated along the trajectory. To recover the entropy production rate, we define the total change in entropy as $\delta S_i = \delta Q/T$, where T is the effective temperature for the process. For the center of mass, we have $T = D_x/2$, which comes from the governing Langevin equation for $x(t)$. Finally, the *rate* of entropy production is the change in entropy over the total length (in time) of the trajectory. We use the same method to calculate the entropy production from the interparticle displacement dynamics and show good agreement in all cases with our analytic results.

We measure the MSD for the center of mass $\langle (x(t) - x(0))^2 \rangle$ by recording $x(t)$ every 10^{-3} time units. We then let dt be a multiple of 10^{-3} that is less than the total simulation time T_{traj} and evaluate the average value of $(x(t+dt) - x(t))^2$ for all $t \in [0, T_{\text{traj}} - dt]$ such that t is also a multiple of 10^{-3}. The effective diffusion coefficient is then given by

$$D_{\text{eff}} = \lim_{t\to\infty} \frac{\langle (x(t) - x(0))^2 \rangle}{2t}. \quad \text{(F2)}$$

[1] M. Mobilia, I. T. Georgiev, and U. C. Täuber, Phase transitions and spatio-temporal fluctuations in stochastic lattice Lotka–Volterra models, J. Stat. Phys. **128**, 447 (2007).

[2] V. N. Biktashev and M. A. Tsyganov, Spontaneous traveling waves in oscillatory systems with cross diffusion, Phys. Rev. E **80**, 056111 (2009).

[3] E. Theveneau, B. Steventon, E. Scarpa, S. Garcia, X. Trepat, A. Streit, and R. Mayor, Chase-and-run between adjacent cell populations promotes directional collective migration, Nat. Cell Biol. **15**, 763 (2013).

[4] K. Hayashi and S.-i. Sasa, The law of action and reaction for the effective force in a non-equilibrium colloidal system, J. Phys.: Condens. Matter **18**, 2825 (2006).

[5] S. Saha, S. Ramaswamy, and R. Golestanian, Pairing, waltzing and scattering of chemotactic active colloids, New J. Phys. **21**, 063006 (2019).

[6] R. Soto and R. Golestanian, Self-assembly of catalytically active colloidal molecules: Tailoring activity through surface chemistry, Phys. Rev. Lett. **112**, 068301 (2014).

[7] J. Agudo-Canalejo and R. Golestanian, Active phase separation in mixtures of chemically interacting particles, Phys. Rev. Lett. **123**, 018101 (2019).

[8] M. Durve, A. Saha, and A. Sayeed, Active particle condensation by non-reciprocal and time-delayed interactions, Eur. Phys. J. E **41**, 49 (2018).

[9] S. A. M. Loos and S. H. L. Klapp, Irreversibility, heat and information flows induced by non-reciprocal interactions, New J. Phys. **22**, 123051 (2020).

[10] S. A. M. Loos, S. M. Hermann, and S. H. L. Klapp, Non-reciprocal hidden degrees of freedom: A unifying perspective on memory, feedback, and activity, arXiv:1910.08372.

[11] A. V. Ivlev, J. Bartnick, M. Heinen, C.-R. Du, V. Nosenko, and H. Löwen, Statistical mechanics where Newton's third law is broken, Phys. Rev. X **5**, 011035 (2015).

[12] S. Saha, J. Agudo-Canalejo, and R. Golestanian, Scalar active mixtures: The nonreciprocal Cahn-Hilliard model, Phys. Rev. X **10**, 041009 (2020).

[13] Z. You, A. Baskaran, and M. C. Marchetti, Nonreciprocity as a generic route to traveling states, Proc. Natl. Acad. Sci. USA **117**, 19767 (2020).

[14] M. Fruchart, R. Hanai, P. B. Littlewood, and V. Vitelli, Non-reciprocal phase transitions, Nature (London) **592**, 363 (2021).

[15] Z. Zhang and R. Garcia-Millan, Entropy production of nonreciprocal interactions, Phys. Rev. Res. **5**, L022033 (2023).

[16] K. Drescher, K. C. Leptos, I. Tuval, T. Ishikawa, T. J. Pedley, and R. E. Goldstein, Dancing *Volvox*: Hydrodynamic bound states of swimming algae, Phys. Rev. Lett. **102**, 168101 (2009).

[17] R. Niu, A. Fischer, T. Palberg, and T. Speck, Dynamics of binary active clusters driven by ion-exchange particles, ACS Nano **12**, 10932 (2018).

[18] F. A. Lavergne, H. Wendehenne, T. Bäuerle, and C. Bechinger, Group formation and cohesion of active particles with visual perception–dependent motility, Science **364**, 70 (2019).

[19] C. H. Meredith, P. G. Moerman, J. Groenewold, Y.-J. Chiu, W. K. Kegel, A. van Blaaderen, and L. D. Zarzar, Predator–prey interactions between droplets driven by non-reciprocal oil exchange, Nat. Chem. **12**, 1136 (2020).

[20] J. Luis-Hita, J. J. Sáenz, and M. I. Marqués, Active motion induced by random electromagnetic fields, ACS Photonics **9**, 1008 (2022).

[21] G. Gardi and M. Sitti, On-demand breaking of action-reaction reciprocity between magnetic microdisks using global stimuli, Phys. Rev. Lett. **131**, 058301 (2023).

[22] H. Alston, A. O. Parry, R. Voituriez, and T. Bertrand, Intermittent attractive interactions lead to microphase separation in nonmotile active matter, Phys. Rev. E **106**, 034603 (2022).

[23] D. Bonazzi, V. Lo Schiavo, S. Machata, I. Djafer-Cherif, P. Nivoit, V. Manriquez, H. Tanimoto, J. Husson, N. Henry, H. Chaté, R. Voituriez, and G. Duménil, Intermittent pili-mediated forces fluidize *nNeisseria meningitidis* aggregates promoting vascular colonization, Cell **174**, 143 (2018).

[24] H. Alston, L. Cocconi, and T. Bertrand, Non-equilibrium thermodynamics of diffusion in fluctuating potentials, J. Phys. A: Math. Theor. **55**, 274004 (2022).

[25] Z. Zhang and G. Pruessner, Field theory of free run and tumble particles in d dimensions, J. Phys. A: Math. Theor. **55**, 045204 (2022).

[26] R. Garcia-Millan and G. Pruessner, Run-and-tumble motion in a harmonic potential: field theory and entropy production, J. Stat. Mech.: Theory Exp. (2021) 063203.

[27] A. P. Solon, M. E. Cates, and J. Tailleur, Active Brownian particles and run-and-tumble particles: A comparative study, Eur. Phys. J.: Spec. Top. **224**, 1231 (2015).

[28] D. Martin, J. O'Byrne, M. E. Cates, E. Fodor, C. Nardini, J. Tailleur, and F. van Wijland, Statistical mechanics of active Ornstein-Uhlenbeck particles, Phys. Rev. E **103**, 032607 (2021).

[29] M. Bothe and G. Pruessner, Doi-Peliti field theory of free active Ornstein-Uhlenbeck particles, Phys. Rev. E **103**, 062105 (2021).

[30] C. Yuan and X. Mao, Asymptotic stability in distribution of stochastic differential equations with Markovian switching, Stochastic Processes Appl. **103**, 277 (2003).

[31] U. Seifert, Stochastic thermodynamics, fluctuation theorems and molecular machines, Rep. Prog. Phys. **75**, 126001 (2012).

[32] L. Cocconi, R. Garcia-Millan, Z. Zhen, B. Buturca, and G. Pruessner, Entropy production in exactly solvable systems, Entropy **22**, 1252 (2020).

[33] C. Bechinger, R. Di Leonardo, H. Löwen, C. Reichhardt, G. Volpe, and G. Volpe, Active particles in complex and crowded environments, Rev. Mod. Phys. **88**, 045006 (2016).

[34] J. R. Howse, R. A. L. Jones, A. J. Ryan, T. Gough, R. Vafabakhsh, and R. Golestanian, Self-motile colloidal particles: From directed propulsion to random walk, Phys. Rev. Lett. **99**, 048102 (2007).

[35] X. Guyon, S. Iovleff, and J.-F. Yao, Linear diffusion with stationary switching regime, ESAIM: Probab. Stat. **8**, 25 (2004).

[36] Z. Zhang and W. Wang, The stationary distribution of Ornstein–Uhlenbeck process with a two-state Markov switching, Commun. Stat. - Simul. Comput. **46**, 4783 (2017).

[37] C. W. Gardiner, *Stochastic Methods: A Handbook for the Natural and Social Sciences*, 4th ed. (Springer, Berlin, 2009).

[38] J. D. Weeks, D. Chandler, and H. C. Andersen, Role of repulsive forces in determining the equilibrium structure of simple liquids, J. Chem. Phys. **54**, 5237 (1971).

[39] A. C. Brańka and D. M. Heyes, Algorithms for Brownian dynamics computer simulations: Multivariable case, Phys. Rev. E **60**, 2381 (1999).

[40] S. A. M. Loos, S. H. L. Klapp, and T. Martynec, Long-range order and directional defect propagation in the nonreciprocal XY model with vision cone interactions, Phys. Rev. Lett. **130**, 198301 (2023).